PHYSICAL REVIEW A VOLUME 19, NUMBER 1 JANUARY 1979

Theory of resonant multiphoton ionization: Application to the cesium atom

Y. Gontier and M. Trahin
Service de Physique Atomique, Centre d'Etudes Nucléaires de Saclay, Boîte Postale No. 2, 91190, Gif-sur-Yvette, France
(Received 27 October 1977; revised manuscript received 19 June 1978)

A quantitative treatment is carried out for the exact operator expressions derived in a previous paper. The formalism of the dressed atom and the concept of level crossings (anticrossings) are used throughout and provide a basis for the quantitative investigation of the resonant three- and four-photon ionization of cesium. The numerical results obtained within this framework are in excellent agreement with experimental observations.

I. INTRODUCTION

Perturbation techniques have been widely used in problems dealing with multiple interactions of radiation fields with atomic systems.[1] Within this framework the transition amplitude corresponding to a definite process is represented by an infinite series in powers of the electric field strength. The successive terms of this series represent the higher-order contributions to the process under consideration.

For moderate intensity one usually retains only the lowest-order term of this series. As an example, the lowest-order contribution to N-photon absorption is given by the term of the series containing exactly N destruction operators of photons. It has been shown in a previous paper,[2] herein referred to as I, that this lowest-order term cannot give a realistic description of any absorption mechanism which involves very intense radiation sources and/or resonant processes. In these cases, one must consider all the higher-order contributions to the process under consideration. It has been shown in I how the whole perturbation series could be exactly summed. Being expressed in terms of continued fractions, the transition amplitudes we have obtained show a rapid convergence at the same time that the perturbation series diverges. In this paper, we consider one of the two circumstances where such expressions for the transition amplitude are to be used, that is, the case of resonant multiphoton absorption induced by radiation fields of moderate intensity.

Extensive use of the results presented in I will be made throughout this paper. The operator expressions derived there will be given an expanded analytical treatment which yields an expression for the time-dependent transition probability. The projector technique[3-5] is used to isolate the resonances inside the continued fractions.

The formalism of the dressed atom as discussed in Ref. 3 has been utilized. It allows giving a consistent description of resonant multiphoton processes. It is shown that the concept of level anticrossing proposed there also holds at optical frequencies when the coupling of the resonant level with the ground state predominates. An example of this case is the three-photon ionization of cesium in an intense field.

In general, we are faced with the alternate situation where the continuum plays the most important role. This comes from the fact that the coupling of the resonant level with the ground state is of higher order. The energy levels concerned with the resonance give rise to a level crossing. Such a phenomenon is illustrated by four-photon ionization of cesium in which there is a three-photon resonance with an intermediate bound state.

The coupling of bound states with the continuum produces an important damping effect which plays a central role in the calculation of the ionization yield. We neglect free-free couplings.

Throughout this paper the occupation number representation is used for the field. Within the intensity range involved here this model for the field is very close to that of an ideal laser. This comes from the fact that for the values of the photon occupation number we consider, the contributions coming from the wings of the Poisson distribution are negligible compared to those centered around its maximum. In other words the Poisson distribution "tends to a δ function."

With regard to the temporal pulse shape, we consider only the case of an adiabatic square pulse.

In order to make a comparison with existing experimental data, the theory is applied to the case of three- and four-photon ionization of cesium. The bound-bound oscillator strengths have been taken from the literature while the bound-free ones have been calculated in the Coulombic model.

Most of the results presented in Sec. III refer to one of the two components of the hyperfine

structure of the ground state. The ones dealing with the other component are obtained through a translation in the photon energy scale.

The principal results obtained in I are summarized in Sec. II where the projector technique is used in the derivation of the resonant transition probability. It is shown how any resonant multiphoton transition can be treated by a three-level model. Some approximate formulas giving the value of the poles and the transition probability are derived. The aim of these formulas is to provide a basis for the discussion of the numerical results presented in Sec. II.

The numerical results of Sec. III supply enough information for a good understanding of the resonance mechanism. The ensemble of results presented there are obtained without introducing the approximations of Sec. II. Three- and four-photon ionization are treated on the same footing.

The energy levels of the dressed atom are first presented. Then the value of the poles are used to calculate the probability. For three-photon ionization, the intensity values are chosen to be larger than the ones usually utilized. This is to enlarge the anticrossing area.

II. THEORETICAL BACKGROUND

A. Projector technique

To calculate the transition probabilities, one needs the matrix elements of the time evolution operator $U(t)$ with respect to the eigenstates of H_0, the free Hamiltonian of the system. These matrix elements have been calculated in I within the framework of the resolvent formalism.[3-5]

For the sake of completeness, the most salient results are summarized below. All the quantities appearing in this section have been already defined in I.

The time evolution operator is given by

$$U(t)=\frac{1}{2\pi i}\oint e^{-izt}G(z)\,dz\,, \tag{2.1a}$$

where

$$G(z)=1/(z-H_0-V)\,, \tag{2.1b}$$

and

$$z=E-i\Gamma\,. \tag{2.1c}$$

The integral of Eq. (2.1a) can be readily performed by the residue theorem once the poles of $G(z)$ are known. This gives rise to the difficult problem of the determination of the poles of $G(z)$. In addition, for resonant processes we are faced with the problem coming from the particular structure of $G(z)$. Thus it was shown in I that the series representing this operator could be expressed in terms of continued fractions.

In the presence of a resonance one or several denominators in the continued fractions vanish. This gives rise to serious complications in the search for the poles. Such a difficulty can be tackled by using a projector technique which yields equivalent expressions where the resonant terms are isolated. Using the notation of Refs. 3 and 4, let P and Q be the projection operators onto and outside of the subspace ϵ spanned by some particular eigenstates of H_0. The projection of $G(z)$ onto ϵ is

$$\tilde{G}(z)=PG(z)P\,. \tag{2.2}$$

From Eq. (2.1b) and owing to the obvious relation $P+Q=1$, it has been shown[3-5] that $G(z)$ is given by

$$\tilde{G}(z)=[z-H_0-\tilde{R}(z)]^{-1}\,, \tag{2.3}$$

where $\tilde{R}(z)$ is the projection of the operator

$$R(z)=V+V\frac{Q}{z-H_0}V+V\frac{Q}{z-H_0}V\frac{Q}{z-H_0}V+\cdots\,, \tag{2.4}$$

onto the subspace ϵ, that is,

$$\tilde{R}(z)=PR(z)P\,. \tag{2.5}$$

It was found in I that the diagonal matrix elements of the operator $R(z)$ are to be calculated from

$$R(z)=V^{+}\bar{\tau}_{\square}\bar{A}\bar{\tau}_0+V^{-}\bar{\tau}_{\square}\bar{B}\bar{\tau}_{\phi}\,, \tag{2.6a}$$

whereas the nondiagonal matrix elements connecting two states energetically separated by a multiple N of the photon energy are to be calculated from

$$R(z)=V^{+}\bar{\tau}_{\square}(\bar{A}\bar{\tau}_0)^{N+1}+V^{-}\bar{\tau}_{\square}(\bar{A}\bar{\tau}_0)^{N-1}\,, \tag{2.6b}$$

where

$$\bar{A}=[Q/(z-H_0)]V^{-}\,, \tag{2.7a}$$

$$\bar{B}=[Q/(z-H_0)]V^{+}\,, \tag{2.7b}$$

$$\bar{\tau}_{\square}=1/(1-\bar{A}\bar{\tau}_0\bar{B}-\bar{B}\bar{\tau}_{\phi}\bar{A})\,, \tag{2.8a}$$

$$\bar{\tau}_0=1/(1-\bar{A}\bar{\tau}_0\bar{B})\,, \tag{2.8b}$$

$$\bar{\tau}_{\phi}=1/(1-\bar{B}\bar{\tau}_{\phi}\bar{A})\,, \tag{2.8c}$$

and

$$V=V^{+}+V^{-}\,. \tag{2.8d}$$

In Eq. (2.6b), the operator $R(z)$ or its conjugate is to be used according to whether the state on the left-hand side of this operator is reached by the absorption or the emission of N photons from the state lying on the right-hand side.

B. Ionization

We proceed now to the derivation of the resonant ionization probability.

In general, a resonance can occur when the energy separation between two atomic levels is approximately equal to an integer multiple m of the photon energy. In the scheme of the dressed atom, the resonance is said to be produced by the crossing (anticrossing) of two (intensity-dependent) energy levels. For brevity, such a resonance will be called an mth order resonance. In this section it is shown that such a concept provides a realistic description of any resonant multiphoton absorption process taking place at optical frequencies.

Let $|g,n\rangle$, $|f,n-N\rangle$, and $|h,n-m\rangle$ be the initial, final, and resonant states, respectively. The atomic states are denoted by $g,f,h,\ldots$ and the radiation states are characterized by their occupation number.

In the cases we consider, the atomic spectrum is not limited to g, f, and h. It is only assumed that the other states do not produce additional resonances. In the reduced notation where $|a\rangle$, $|b\rangle$, and $|c\rangle$ stand for $|g,n\rangle$, $|f,n-N\rangle$, and $|h,n-m\rangle$, respectively, we have to calculate $G_{ba}(z)$. This task can be accomplished by inverting the 3×3 matrix $[z-H_0-R(z)]$.

The determination of the complex poles is very tedious and the calculation of the probability involves unessential manipulations of high-order bound-free matrix elements of $R(z)$.

For these reasons, we prefer to use an alternate method which is based upon the well-known unitary property of $U(t)$.[6,7] One readily finds that the probability for the atom to be ionized at time t is

$$|U_{ba}(t)|^2 = 1 - |U_{aa}(t)|^2 - |U_{ca}(t)|^2, \tag{2.9}$$

which accounts for probability conservation.

In calculating the ionization probability by using Eq. (2.9) one has to consider only the bound-bound matrix elements of $G(z)$. The whole contribution of the continuum is taken into account within the matrix elements of $G(z)$ by integration (see Appendix B).

It can be easily shown that the relevant matrix elements of $G(z)$ occurring in Eq. (2.9) are given by

$$G_{aa}(z) = [z - E_c - \underline{R}_{cc}(z)] \Big/ \{[z - E_a - \underline{R}_{aa}(z)] \times [z - E_c - \underline{R}_{cc}(z)] - \underline{R}_{ac}(z)\underline{R}_{ca}(z)\}, \tag{2.10a}$$

$$G_{ca}(z) = \underline{R}_{ca}(z) \Big/ \{[z - E_a - \underline{R}_{aa}(z)] \times [z - E_c - \underline{R}_{cc}(z)] - \underline{R}_{ac}(z)\underline{R}_{ca}(z)\}, \tag{2.10b}$$

where

$$\underline{R}(z) = R(z) + R(z) \int \frac{|b\rangle\langle b|}{z - E_b - R_{bb}(z)} dE_b R(z). \tag{2.10c}$$

The density of states is taken into account through a suitable normalization of the wave functions of the continuum. The important consequence of the integration is that, in contrast to what happens in the case of bound-bound transitions taking place between infinitely sharp levels, the poles a and c depart from the real axis. In other words, the coupling of the states $|a\rangle$ and $|c\rangle$ with the continuum gives rise to a broadening (intensity dependent) of these levels. This is easily shown by noting that the integral occurring in Eq. (2.10c) can be calculated to a good approximation by using the identity

$$\lim_{\eta\to 0} \frac{1}{E - E_b - R_{bb} - i\eta} = \mathcal{P}\frac{1}{E - E_b - R_{bb}} + i\pi\delta(E - E_b - R_{bb}), \tag{2.11}$$

where the principal-part integral is evaluated at $E - R_{bb}$.

In Eq. (2.11) it is supposed that R_{bb} is real. In general, R_{bb} is complex. This is due to integrations over the continuum variables of states containing different numbers of photons. It is clear that since these complex quantities appear in the successive denominators of the continued fractions of $R(z)$, they are of higher order compared to the one calculated from Eqs. (2.10c) and (2.11). Thus in a first approximation they are not taken into account and the complex part of $\underline{R}(z)$ is derived from Eq. (2.10c) by assuming that R_{bb} is a function of a real variable.

From Eq. (2.9), one sees that the mechanism of resonant ionization is discussed in terms of the behavior of a two-level system with intensity-dependent losses.[8] The number of ions created is equal to the depletion of the populations of the levels a and c caused by the coupling of these states with the continuum. As will be shown in Sec. III this number increases with time and tends to N_0 the number of atoms contained in the interaction volume at time $t=0$. In spite of its apparent simplicity, Eq. (2.9) gives rise to serious computational difficulties. The reason is that the transition probability under consideration is given by the difference between quantities which are very near to each other, i.e., $|U_{aa}|^2 + |U_{ca}|^2 \simeq 1$. The results are found to be very sensitive to the value of the matrix elements of $R(z)$. Only the accurate quantitative treatment of Sec. III makes it possible to find a reliable enough result for the transition probability.

We proceed now with the derivation of formulas

which will be useful for the discussion of the numerical results.

The equations giving the real and imaginary parts of the poles in the anticrossing region are straightforwardly derived from Eqs. (2.10a) and (2.10b). They are found to be

$$(E-\tilde{E}_a)(E-\tilde{E}_c)-(\Gamma-\Gamma_{aa})(\Gamma-\Gamma_{cc})-(\Delta_{ac}^2+\Gamma_{cc}^2)=0\,, \tag{2.12a}$$

$$\Gamma=[\Gamma_{cc}(E-\tilde{E}_a)+\Gamma_{aa}(E-\tilde{E}_c)]/(2E-\tilde{E}_a-\tilde{E}_c)\,, \tag{2.12b}$$

where

$$\Delta_{ij}(E,\Gamma)=\mathrm{Re}[\underline{R}_{ij}(z)]\,, \tag{2.13a}$$

$$\Gamma_{ij}(E,\Gamma)=\mathrm{Im}[\underline{R}_{ij}(z)]\,, \tag{2.13b}$$

and

$$\tilde{E}_i(E,\Gamma)=E_i+\Delta_{ii}(E,\Gamma)\,. \tag{2.13c}$$

Equations (2.12) and (2.13) show that the only accurate determination of the complex energies of the dressed atom can be made numerically. Nevertheless, in the limit where $\Delta_{ij}(E,\Gamma) \to \Delta_{ij}(E_i,\Gamma_{ii})$ and $\Gamma_{ij}(E,\Gamma)\to\Gamma_{ij}(E_i,\Gamma_{ii})$, Eq. (2.12a) simplifies and becomes a fourth-order equation in E. As is shown in Appendix A there are only two solutions, which are given by

$$E^{\pm}=\tfrac{1}{2}(\tilde{E}_a+\tilde{E}_c)\pm(D_{ac}^2+Q_{ac}^2)^{1/4}\times[\tfrac{1}{2}+\tfrac{1}{2}D_{ac}/(D_{ac}^2+Q_{ac}^2)^{1/2}]^{1/2} \tag{2.14a}$$

and

$$\Gamma^{\pm}=\tfrac{1}{2}(\Gamma_{aa}+\Gamma_{cc})\mp(D_{ac}^2+Q_{ac}^2)^{1/4}\times[\tfrac{1}{2}-\tfrac{1}{2}D_{ac}/(D_{ac}^2+Q_{ac}^2)^{1/2}]^{1/2}\,, \tag{2.14b}$$

where D_{ac} and Q_{ac} are defined by Eqs. (A8a) and (A8b).

Owing to Eqs. (2.10) one readily finds

$$U_{aa}(t)=\frac{E^+-E_c-\Delta_{cc}^+-i(\Gamma^+-\Gamma_{cc}^+)}{E^+-E^--i(\Gamma^+-\Gamma^-)}\,e^{-iE^+t}e^{-\Gamma^+t}+\frac{E^--E_c-\Delta_{cc}^--i(\Gamma^--\Gamma_{cc}^-)}{E^--E^+-i(\Gamma^--\Gamma^+)}\,e^{-iE^-t}e^{-\Gamma^-t}\,, \tag{2.15a}$$

$$U_{ca}(t)=\frac{\Delta_{ca}^+-i\Gamma_{ca}^+}{E^+-E^--i(\Gamma^+-\Gamma^-)}\,e^{-iE^+t}e^{-\Gamma^+t}+\frac{\Delta_{ca}^+-i\Gamma_{ca}^-}{E^--E^+-i(\Gamma^--\Gamma^+)}\,e^{-iE^-t}e^{-\Gamma^-t}\,, \tag{2.15b}$$

where

$$\Delta_{ij}^{\pm}=\Delta_{ij}(E^{\pm},\Gamma^{\pm})\,, \tag{2.15c}$$

$$\Gamma_{ij}^{\pm}=\Gamma_{ij}(E^{\pm},\Gamma^{\pm})\,. \tag{2.15d}$$

From Eqs. (2.9) and (2.15) the ionization probability can be put in the form

$$P(t)=1-\alpha^+e^{-2\Gamma^+t}-\alpha^-e^{-2\Gamma^-t}+2\left(C_1\frac{\cos(E^+-E^-)t}{(E^+-E^-)^2+(\Gamma^+-\Gamma^-)^2}+C_2\frac{\sin(E^+-E^-)t}{(E^+-E^-)^2+(\Gamma^+-\Gamma^-)^2}\right)e^{-(\Gamma^++\Gamma^-)t}\,, \tag{2.16}$$

where

$$\alpha^{\pm}=\frac{\Omega_{cc}^{\pm2}+\Delta_{ca}^{\pm2}+\gamma_{cc}^{\pm2}+\Gamma_{ca}^{\pm2}}{(E^+-E^-)^2+(\Gamma^+-\Gamma^-)^2}\,, \tag{2.17a}$$

$$C_1=\Omega_{cc}^+\Omega_{cc}^-+\Delta_{ca}^+\Delta_{ca}^-+\gamma_{cc}^+\gamma_{cc}^-+\Gamma_{ca}^+\Gamma_{ca}^-\,, \tag{2.17b}$$

$$C_2=\Omega_{cc}^+\gamma_{cc}^-+\Delta_{ca}^+\Gamma_{ca}^--\gamma_{cc}^+\Omega_{cc}^--\Gamma_{ca}^+\Delta_{ca}^-\,. \tag{2.17c}$$

In Eqs. (2.17) $\Omega_{cc}^{\pm}$ and $\gamma_{cc}^{\pm}$ are defined by

$$\Omega_{cc}^{\pm}=E^{\pm}-E_c-\Delta_{cc}^{\pm} \tag{2.18a}$$

and

$$\gamma_{cc}^{\pm}=\Gamma^{\pm}-\Gamma_{cc}^{\pm}\,. \tag{2.18b}$$

Apart from a difference in notation, it can be shown that the above expressions are in agreement with the ones obtained by Beers and Armstrong[6] in the case of two-photon ionization.

Before ending this section it should be noted that the group of formulas we have derived are useful because they give much information about the behavior of the probability. Nevertheless they are not used in the quantitative discussion of Sec. III. The reason is that the value of the probability is very sensitive to the precision utilized in the calculation of the quantities appearing in the formulas.

III. NUMERICAL RESULTS

A. General considerations

This section is devoted to a careful quantitative analysis of the operator expressions found in I. To allow ample space for the numerical results, the computational techniques used will be only mentioned or briefly described when necessary. No approximations like the ones discussed in Sec. II are invoked in carrying out the present numerical analysis so as to obtain the most accurate results for each particular basis of atomic states considered. The atomic model involved in the following discussion is set up from a finite number of discrete levels and a single continuum. The theory is illustrated by the three- and four-photon ionization of the cesium atom. The advantage of working with an alkali atom is that the intensity of the radiation field required for multiple

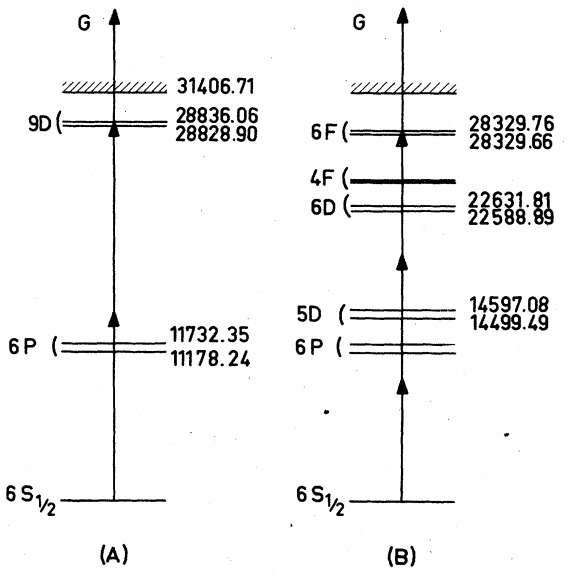

FIG. 1. Spectra of the Cs atom utilized for the calculation of (a) three- and (b) four-photon ionization.

absorption is low enough to make our atomic model relevant. At such intensities it is found that those contributions of the continued fraction accounting for high-order absorption and emission of photons in the continuum are not significant. Thus, in this case, sufficient accuracy is obtained with this single continuum approximation (SCA). Regarding the discrete spectrum, the number of levels entering into the calculation is determined by the wavelength of the light. This is exemplified in Fig. 1 where the spectra of the Cs atom used for three- and four-photon ionization are shown. These resonant situations are chosen because they have been experimentally investigated.[9-11]

The resonant level for three-photon ionization is the $9D_{3/2}$ whereas the one providing the main contributions to the resonance for four-photon ionization is the $6F_{5/2}$.

One observes in Fig. 1(a) that only the $9D$ and $6P$ doublets have been retained in the calculations. The other levels are far enough to give negligible contributions to the shift of the ground state and to the transition amplitude.

A slightly different situation occurs in Fig. 1(b) where the $5D$ and $6D$ doublets are located on both sides of the two-photon virtual level. They introduce contributions of the same order of magnitude and thus they must both be included in the calculations. The $4F$ doublet is also included since the calculations of R_{ab} involves F levels (as a consequence of the projector technique, the $6F$ doublet is excluded from the ensemble of states entering into this calculation). The bound-bound oscillator strengths have been taken from the literature.[12] The values not reported in the literature have been computed by using the Coulomb approximation, i.e., $(6D_{3/2} - 6F_{5/2}) \rightarrow 0.13$; $(6D_{5/2} - 6F_{5/2}) \rightarrow 0.011$; $(6D_{5/2} - 6F_{7/2}) \rightarrow 0.23$.

To perform all the relevant integrals over the continuum, the required bound-free matrix elements have been obtained from a Coulombic model. This we believe is justified for the high-energy levels. Thus, from the energy of the $6F$ state, an effective nuclear charge Z_e is determined and is used to evaluate the electronic wave functions. The value of the photoionization cross section of the $6F$ state calculated by this method is 1.01×10^{-18} cm^2. It is very near to 1.4×10^{-18}, the value obtained by Aymar[13] from a more sophisticated potential model.

One must note that, in our case, the quantum-defect method does not provide better results. The knowledge of the cesium spectrum regarding the G states is not sufficient for the calculation of a reliable value of the quantum defect of these states. From the only $5G$ and $6G$ states whose energies are known, one observes that the quantum defect is very small and does not vary slowly with the principal quantum number $n(\mu_{6G}/\mu_{5G} = 7.6)$.

Obviously, more realistic oscillator strengths derived from a reliable model potential could improve our results. But the agreement observed between our Coulombic oscillator strength and other experimental and theoretical data reinforces our confidence in the parameters we use.

One must note that the position of the poles of $G(z)$ does not depend on the dimension of ϵ. This obvious property is very useful because the poles can be calculated by considering suitable two-dimensional subspaces.

In every case the poles are determined with the help of standard iterative techniques based on the changes in sign of the energy-dependent functions. Thus the value of the energy is known up to an arbitrary degree of accuracy.

The behavior of the energy levels of the dressed atom is illustrated in Fig. 2 for resonant three-photon ionization of cesium. The wavelength of the radiation is such that the energy separation between the $9D_{3/2}$ state and the ground state is approximately equal to the energy of two photons in the absence of a level shift (static detuning). The photon energy E_p corresponding to the exact resonance is 14 414.45 cm^{-1} for the component of the hyperfine structure of the ground state we have chosen. To show the anticrossing which takes place in this third-order process without resorting to a prohibitive expansion of the scales, the values of the intensity are somewhat larger than the ones usually involved in the experiments.

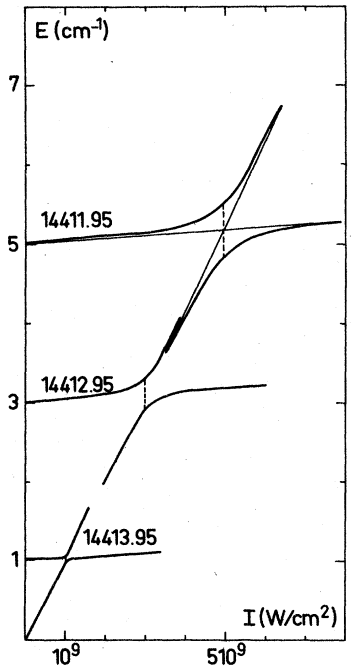

FIG. 2. Energy of the dressed atom as a function of the intensity for the second-order resonance on the $9D_{3/2}$ level in a three-photon ionization of Cs. The dashed lines give the distance between the poles at the anticrossing point which is determined by the asymptotes of the hyperbolas.

The unperturbed energy of the ground state is chosen to be the origin of the energy scale. The pairs of curves correspond to particular resonant situations obtained by varying the frequency of the radiation.

The three pairs of curves represent the energy levels when the photon energy is successively increased by 0.5, 1.5, and 2.5 cm^{-1} from this initial value. For this two-photon resonance the initial detuning is twice the above photon energy jumps.

The most salient feature of the curves presented in Fig. 2 is that the energy levels in every pair do not cross each other. In considering the different solutions of Eqs. (2.14) (see Appendix A), it can be shown that this property holds as long as $(\Gamma_{aa}-\Gamma_{cc})^2<4|\underline{R}_{ac}|^2$. Near the resonance $\tilde{E}_a$ and $\tilde{E}_c$ exhibit linear variations with regard to the intensity. At low intensity the corresponding curves are the asymptotes for the hyperbola representing the energy E^+ and E^-.[3]

This is illustrated in Fig. 2 where a linear scale for the energy has been adopted to have an expanded representation of the phenomenon. The difference E^+-E^- which is found to be minimum for the intensity corresponding to the crossing between the asymptotes, i.e., $\tilde{E}_a-\tilde{E}_c=0$, plays a central role in the expression of the probability. One can see, for example, from the approximate expression of Eq. (2.16) that the probability is inversely proportional to powers of this quantity. Therefore, the smaller is the difference E^+-E^-, the greater is the enhancement of the transition probability.

Such an interpretation of resonance in terms of the crossing (anticrossing) of levels describes the role played by the damping of the resonance curve produced by the intensity-dependent coupling of the resonant state with the ground state and with the continuum.

The difference E^+-E^- taken at the anticrossing point provides the value of the damping coming from the ground state. Such a damping is important at the early stage of the process, i.e., for very short time. In this case the damping caused by time-dependent exponentials is not appreciable. For the time intervals involved here (few nanoseconds) the effect of the exponentials is very sensitive. In fact, the behavior of the resonant-ionization processes under consideration is essentially governed by these exponentials. The broadening of the resonance curves comes from the damping they provide as long as the coupling of the resonant level with the ground state is small (moderate intensity).

Calculations have been performed at low intensity. The anticrossing point has been located from the examination of curves analogous to the ones shown in Fig. 2. We have found that at $I=10^7$ W/cm^2 the anticrossing point (dynamic resonance) is shifted by 5.10^{-3} cm^{-1}.

From the discussion of Appendix A, a crossing or an anticrossing appears according to whether the coupling between the ground state and the resonant state is smaller or larger than the coupling of this resonant state with the continuum. Since at optical frequencies these couplings are of high order, the situation can change as the intensity is varied and a crossing (anticrossing) can evolve towards an anticrossing (crossing). This phenomenon is not observed in three-photon ionization since the two competing couplings are of second order. Thus the levels will always show an anticrossing. But such changes can be observed in four-photon ionization, for example.

We have represented in Fig. 3 the real part of the energy of the dressed atom for resonant four-photon ionization of Cs.

Within the range of intensity values considered, we are concerned with a $6F_{5/2}$-$6S_{1/2}$ crossing. It is found that for intensity values greater than 1.1×10^{12} W/cm^2 this crossing becomes an anticrossing. The photon energy giving rise to the static resonance is 9443.254 cm^{-1}. The photon

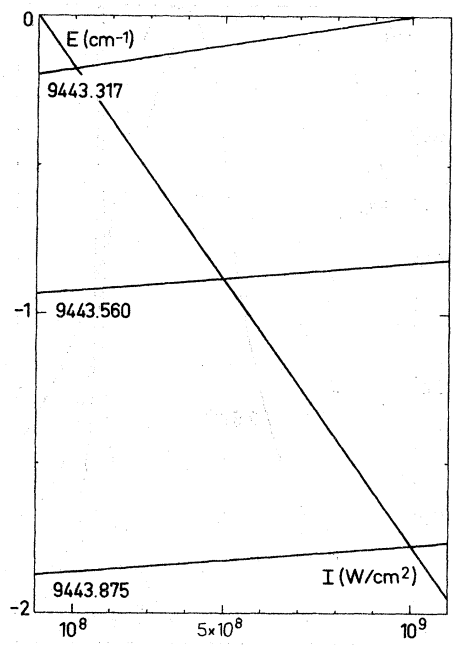

FIG. 3. Energy of the dressed atom as a function of the intensity for the third-order resonance on the $6F_{5/2}$ level in a four-photon ionization of Cs. As in Fig. 2, the energy of the ground state is chosen to be the origin of the energy scale.

energies corresponding to the three pairs of curves are such that the crossing takes place at $I = 10^8$, 5×10^8, and 10^9 W/cm^2, respectively. As is shown in Figs. 1 the relative position of the first virtual level (one-photon) and the nearest ($6P$) atomic levels is inverted. Therefore, the sign of the shift of the ground state is changed with regard to that which is found in three-photon ionization. In the representation of Fig. 3 where the unperturbed energy of the ground state is taken as the origin of the energy, the crossing is found to take place in the lower half-plane.

To make a comparison between theory and experiment,[10] the intensity values are taken within the range 10^8 to 10^9 W/cm^2. These values are relatively low compared to the ones utilized in Fig. 2. This explains the differences shown by the curves presented in Figs. 2 and 3. In particular, the anticrossing of Fig. 2 is replaced by a crossing. This is principally due to the smallness of the coupling of the $6F$ state with the ground state. From the curves shown in Fig. 3, it is clear that for such a resonance,[14] the position of the crossing point is principally governed by the behavior of the ground state with regard to the intensity and the photon energy.

B. Calculation of the probability

From the knowledge of the poles of $G(z)$ it is possible to calculate the transition probability. This is numerically done for resonant three- and four-photon ionization of Cs.

Since the quantity we calculate is the probability that a single atom is ionized at the end of the pulse, the number of ions thus created is N_0 times this probability, if N_0 is the number of atoms present in the interaction volume at $t = 0$. Before discussing the numerical results, we briefly indicate how the calculations have been handled.

As before the convergence of the continued fractions has been checked at each step of the calculation. The subspace previously defined contains all the quasiresonant atomic states, each of them being associated with the nearest field state. This precaution allows the avoidance of possible quasiresonances which could give rise to difficulties in the calculation of the continued fractions when the intensity is varied. The alternative to this procedure is to increase the size of the matrices involved in the calculations. On the other hand, the computational expressions for the transition probability are somewhat lengthened compared with the ones shown in Eq. (2.16).

To simplify the discussion, only the case of an adiabatic square pulse is considered.[15] Within this approximation, one deals with a single-mode field. The introduction of more realistic pulse shape into the calculations needs a special treatment which will be examined later.[13] Concerning the time dependence, it is found that the oscillatory character of the probability predicted by Eq. (2.16) doesn't appear in the results presented here. The reason is that, in the examples under consideration, the damping arising from the coupling of the resonant level with the continuum is strong enough to avoid any significant oscillation of the probability. This property is exhibited in Figs. 4 and 5 which represent the time variation of the probability for three- and four-photon ionization, respectively. The curves which are drawn for some typical values of the photon energy are remarkably smooth. Starting from zero, they quickly increase and then they tend to unity (saturation). One observes that the saturation regime is rapidly reached at high intensity and for small static detuning. This explains, for example, the rapid variations of the curves of Fig. 4 which correspond to an intensity value (2.8×10^9 W cm^{-2}) which is somewhat larger than the ones usually used in three-photon processes induced by nanosecond pulses.

The dispersion curves for three-photon ionization are shown in Fig. 6 for the intensity values

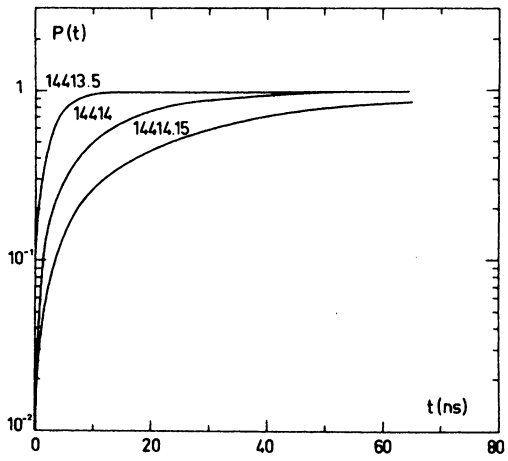

FIG. 4. Three-photon ionization probability as a function of time for three values of the photon energy ($I=2.8\times10^{9}$ W/cm^2, dynamic resonance at $E_p=14\,413.05$ cm^{-1}).

previously utilized. Obviously, the important distortions of the maxima are due to the saturation. To reduce its effect the interaction time is shortened and chosen to be 10 nsec. The energy interval where such a flattening takes place increases with the intensity.

At the same time, the shift and the width of the resonance curves become more and more important. It is to be noted that the variations of the width are more rapid than the ones shown

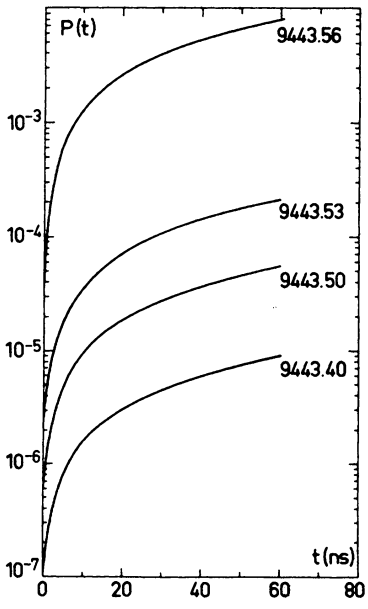

FIG. 5. Four-photon ionization probability of Cs as a function of time for four near-resonant photon energies ($I=5\times10^{8}$ W/cm^2, dynamic resonance at $E_p=9443.565$ cm^{-1}).

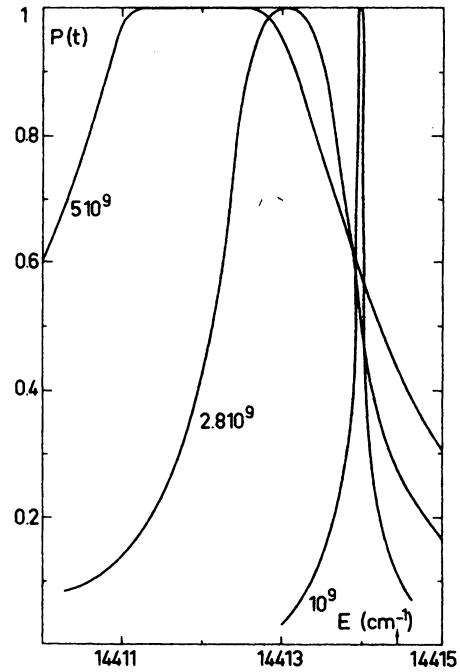

FIG. 6. Three-photon ionization dispersion curves of Cs. The number beside the curves denotes the intensity in W/cm^2. Interaction time is 10 nsec and the arrow gives the position of the static resonance on the $9D_{3/2}$ level ($E_p=14\,414.45$ cm^{-1}).

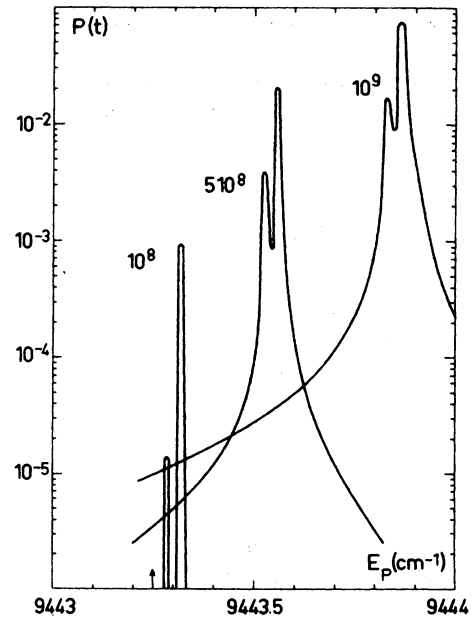

FIG. 7. Four-photon ionization probability of Cs as a function of the photon energy. The intensity is written beside the curves. The interaction time τ is 50 nsec and the arrow indicates the position of the static resonance on the $6F_{5/2}$ level ($E_P=9443.254$ cm^{-1}).

by the shift. Thus, in contrast to the shift whose variation is approximately linear with regard to the intensity, the width of the resonance curves is given by a more complicated law.

The resonance curves for four-photon ionization of cesium are shown in Fig. 7. The intensity values and the interaction time (50 nsec) are chosen to be those usually utilized in nanosecond experiments.[10] Under these circumstances the calculations are performed far from the saturation condition. One finds that the maxima are well resolved for the two components of the $6F$ doublet.

As before, the effect of the intensity is to shift and to broaden the resonance curves. The shift is again linear in intensity, its magnitude is in excellent agreement with the experimental values shown in Fig. 10(b) of Ref. 10 and with those of Ref. 11 which are reported in Fig. 8. The slight discrepancy which is observed at high intensity comes from spatial effects which take place in the interaction volume near saturation. This particular aspect of the problem will be examined later.

To limit the size of the figure, the wings of the curves of Fig. 7 have been truncated. Since in most cases we are interested in the position and the amplitude of the resonance peaks they have been plotted in Figs. 9 and 10 against the resonance detuning for three typical interaction times. The dashed lines indicate the corresponding value of the intensity which is to be read on the right-hand-side scale. These curves are interesting because they are drawn for a wide range of values of the detuning and the intensity. On the other hand, they are independent of the origin of the energy scale. Thus, they can be invoked in any discussion dealing with the hyperfine structure of the ground state. For example, one observes in Fig. 9 that at $I = 10^7$ W/cm^2 the detuning of the resonance is about 10^{-2} cm^{-1}. In the photon scale, this corresponds to a variation of the photon energy of 5×10^{-3} cm^{-1} because we are faced with a second-order resonance. In taking into account the hyperfine structure of the ground state, one finds that two resonance conditions can be fulfilled. Assuming that the resonances take place between undisplaced levels (static resonances), one finds that the photon energies must be 14 414.295 and 14 414.450 cm^{-1}. Since the resonances are shifted towards small photon energies (see Fig. 6), two (dynamic) resonances can be observed at $E_p^{(1)} = 14\,414.290$ cm^{-1} and $E_p^{(2)} = 14\,414.445$ cm^{-1}.

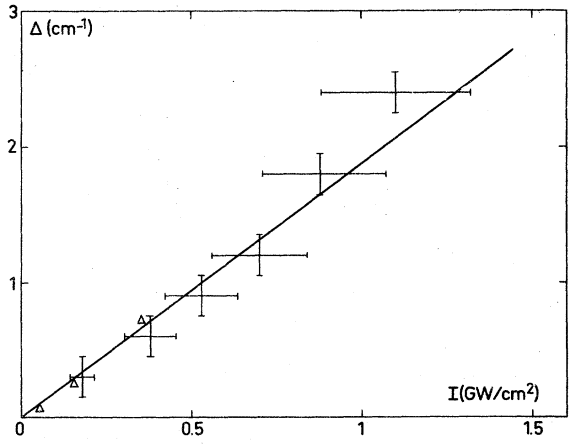

FIG. 8. Shift of the resonance peak for four-photon ionization of Cs as a function of the intensity. The full line represents the results obtained from the present work. The experimental data are those of Ref. 10 (triangles) and Ref. 11 (crosses).

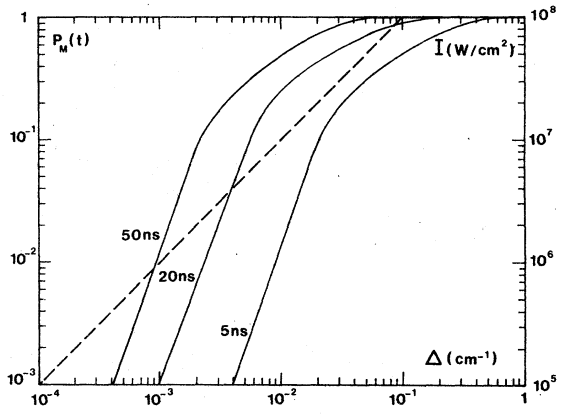

FIG. 9. Maximum probability as a function of the resonance detuning for three-photon ionization of Cs. The amplitude of the peaks (full lines) are to be read on the left-hand-side scale. The dashed line gives the value of the resonance detuning as a function of the intensity whose value is to be read on the right-hand-side scale. The number above the curves is the interaction time.

In comparing with the experimental results of Ref. 9, one sees that the first resonance lies within the experimental error bars. In addition, from an interpolation of the curves of Fig. 9 one finds that the maximum probability for a pulse duration of 40 nsec is equal to 0.35. This value is in good agreement with the experimental one, but owing to the experimental uncertainty, the only reasonable conclusion which can be drawn is: both experiment and theory predict that for this intensity value the saturation regime is not reached whereas more than 10% of atoms have been ionized. This discussion emphasizes the usefulness of the curves of Figs. 9 and 10.

The last remark which can be formulated about the results presented in this section refers to the

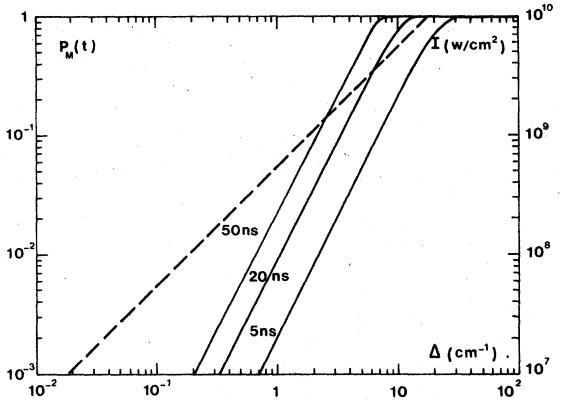

FIG. 10. Maximum probability as a function of the resonance detuning for four-photon ionization of Cs (full lines and left-hand-side scale). As in Fig. 9, the dashed line gives the value of the detuning as a function of the intensity (right-hand-side scale).

behavior of the probability near resonance. From Eq. (2.16), the probability which is inversely proportional to the square of the distance between the poles $(E^+ - E^-)$ seems to be essentially governed by such denominators. In fact, the mechanism is somewhat more complicated. It can be shown from Eq. (2.14b) that $\Gamma^{\pm}$ have a resonant structure, their maxima being centered at the anticrossing point. Therefore, in Eq. (2.16) the damping originated by the time-dependent exponentials becomes more and more important as the resonance is tuned, i.e., as the difference $E^+ - E^-$ becomes small. These effects combine themselves and one observes that for the interaction times we consider the enhancement provided by the resonant denominators is seriously limited by the damping coming from the exponentials.

This is illustrated in Fig. 11 where the quantities $|E^+ - E^-|$ and Γ^+ have been plotted against the photon energy for three-photon ionization. As was previously mentioned, Γ^+ shows a maximum at the anticrossing point, i.e., when $|E^+ - E^-|$ is minimum.

The last comparison which is to be made between the theory and the experiments deals with the variation of the probability as a function of the intensity. It is that variation which is most thoroughly studied in the experiments.

In Fig. 12, the value of the probability for four-photon ionization is plotted against the intensity for some typical photon energies. These energies are located on both sides of 9443.25 cm^{-1} which corresponds to a resonance on the $6F_{5/2}$ level in the absence of level shifts (static resonance).

As was found in hydrogen[16] each of the curves

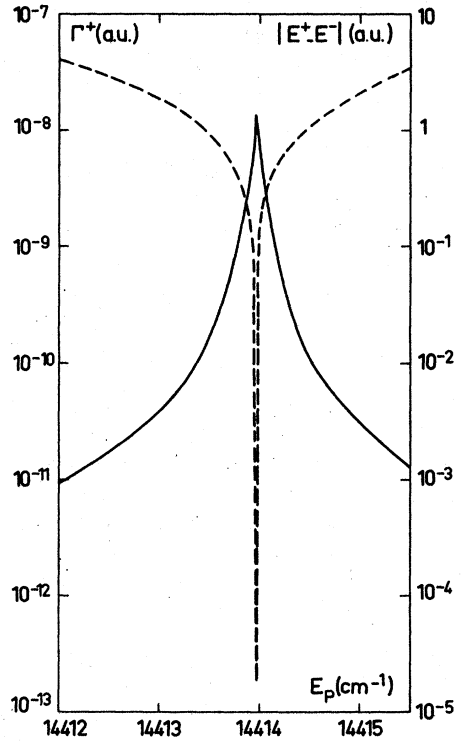

FIG. 11. Plot of Γ^+ (full line and left-side scale) and $|E^+ - E^-|$ (dashed line and right-side scale) as functions of the photon energy.

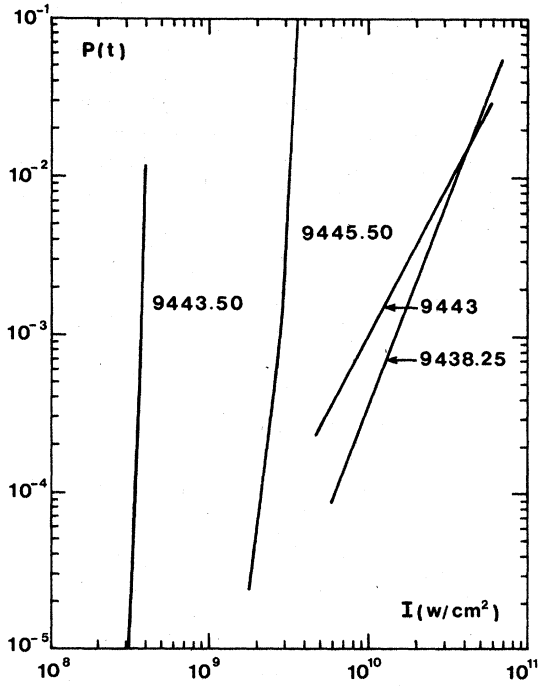

FIG. 12. Resonant four-photon ionization of Cs vs the intensity ($\tau = 50$ nsec). The numbers beside the curves indicate the photon energy in cm^{-1}.

show a resonance peak for a well-defined value of the intensity. In experiments, the valleys of the curves are not observed. The reason is to be found in the spatial effects which take place in the interaction volume. These effects come from the geometry of the beam. All the regions of the interaction volume "do not see" the same intensity. Therefore, the small elementary cells of the focal volume are successively submitted to resonance conditions as the intensity varies. The consequence of such a phenomenon is that the experimental curves do not show any decreasing part. Thus for the sake of clarity only the ascending branches of the curves have been reported in Fig. 12.

We see that the slopes of the curves depart from 4, the value they take far from resonance. On the other hand, for negative detunings, the variations of the probability are more rapid than the ones observed in the zone of positive detunings. This property appears more clearly by calculating the ratio of the increase of the probability over the corresponding intensity interval, i.e., by calculating the order of nonlinearity $K = [d \log P(t)]/(d \log I)$ (Ref. 10). Figure 13 shows the variation of K as a function of the resonance detuning for this four-photon ionization process. Owing to the experimental situation the curve is drawn for a well-defined value of the probability (and thus the ion number) which is chosen to be far from the saturation [$P(t) = 10^{-3}$ for $t = 50$ nsec]. The agreement between the experimental (Fig. 7 of Ref. 10) and theoretical results is highly satisfactory. As was previously observed in hydrogen[16] and in the cesium atom,[17] the order of nonlinearity exhibits important variations near resonance. In the present case, the curves are strongly asymmetric as we cross the static resonance. The important point to be noted is the rapid and important variation of the order of nonlinearity for small resonance detuning. Thus within a small energy interval the lowest value of K is about 2 whereas its upper bound is greater than 30. This is the consequence of the particular behavior of the poles of $G(z)$ in the crossing region predicted by our theory. To see this we have represented in Fig. 14, the energy of the dressed atom as a function of the intensity for two photon energies lying on both sides of the one giving rise to the static resonance, namely, 9443.082 and 9443.418 cm^{-1}.

From the discussion of the preceding section, we know that the behavior of the probability is essentially governed by the quantity $E^+ - E^-$, i.e., the distance between the poles. Thus, from the variations of this distance with regard to the intensity, it is possible to get some insight into the rate of growth of the probability near the crossing point. For example, in Fig. 14 one sees that the relation $AB/A'B' \gg AC/A'C'$ holds for any value of the intensity near the one corresponding to the crossing. Therefore, the most important variations of the probability will take place in the crossing area, i.e., in the region of negative detuning. This is in agreement with what is found in terms of the accurate calcula-

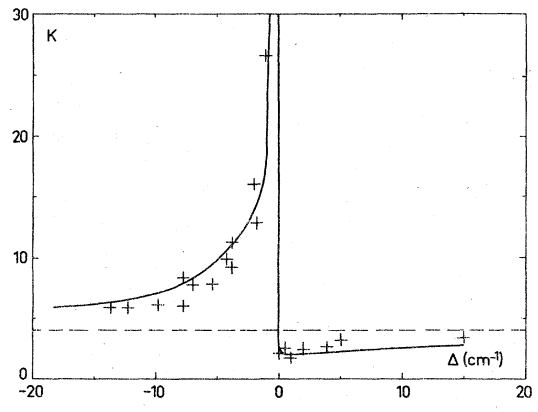

FIG. 13. Order of nonlinearity for four-photon ionization of Cs vs the resonance detuning as calculated from the present work (full line) ($\tau = 50$ nsec). The crosses represent the experimental data of Ref. 10.

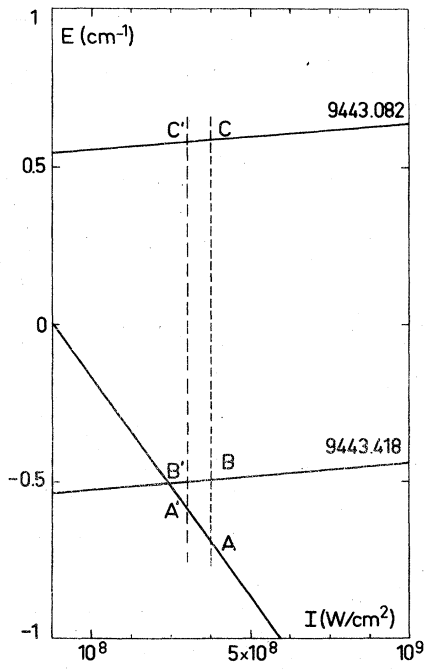

FIG. 14. Energy of the dressed atom corresponding to equal resonance detunings of opposite signs in the case of four-photon ionization of Cs.

tion whose results are summarized in Fig. 13. Roughly speaking, the change in the variation of the probability is due to the sudden disappearance of the dynamic resonance as one crosses the static resonance. It is clear that the greater the angle between the curves representing the energy levels giving rise to the crossing, the greater are the variations of the probability. As a consequence, the asymmetry is expected to be important for atoms in which the ground state is strongly coupled with the other states. The cesium atom provides such an example. The experimental verification of such a behavior reinforces our confidence in the reliability of the present numerical application of the theory presented in I.

IV. CONCLUSION

The aim of this paper was to present a quantitative analysis of resonant-ionization processes induced by radiation fields of moderate intensity. It demonstrates how the operator expressions for the transition probability, which we obtained in a previous paper, can be used.

Within the dressed-atom formalism, the projector technique allowed the elimination of the resonances in the continued fractions, which is the principal source of difficulties in such a calculation.

Three- and four-photon ionization of cesium are discussed at length in Sec. III.

The method used for the determination of the probability shows the role played by the saturation effects. As was shown in the experiments, this saturation depends on the intensity, the interaction time and the resonance detuning. The calculations have been performed for a wide range of variation of these quantities.

The position and the amplitude of the resonance peaks have been calculated when the intensity and the photon energy are varied. As a result of accurate calculations it was found that within the range of intensity values 10^7–10^{10} W/cm^2, the shift of the resonance shows linear variations with respect to the intensity. In contrast to what happens with their shifts, the amplitudes of the peaks are very sensitive to higher-order effects. In fact, we have observed that the shift of the resonance is essentially governed by that of the ground state. The crossing (anticrossing) point moves on the straight line representing the energy of the ground state.

In spite of the usual uncertainty on the value of the oscillator strengths and on the experimental measurements, the agreement between theory and experiment is shown to be remarkably good throughout this paper. The reason for such agreement is believed to be the exact treatment of the perturbation series in I and in the accurate numerical exploitation of the results obtained from there.

Nevertheless, the numerical results can be improved by replacing the adiabatic square pulse by a more realistic pulse shape and by calculating the number of ions produced in the whole interactions volume. These effects which can be taken into account from a simple generalization of the results presented here will be discussed later.

The statistical model for the single-mode field adopted here is that of an ideal laser field. The reason is that most of the nanosecond experiments have been performed by using radiation sources which are well represented by this model.

The last important remark which can be made is that the standard concept of a time-independent cross section which has been intensively invoked in the past decade must be replaced by that of a time-dependent probability or time-dependent absorption coefficient. From a discussion like the one presented here, the notion of a time-independent transition rate can be seen to be inadequate. The transition probability becomes a complicated function of time which shows damped Rabi oscillations.

The advantage deriving from the added complication is that we have a realistic model which permits a consistent discussion of any multiphoton process.

ACKNOWLEDGMENTS

The authors would like to acknowledge pertinent remarks from Professor C. Cohen-Tannoudji and many valuable discussions with Dr. C. Manus, Dr. G. Mainfray, Dr. J. Morellec, and Dr. L. Lompre concerning the experimental aspects of the problem. They are indebted to Professor S. Geltman for pointing out many improvements in an earlier version of this paper.

APPENDIX A

By using Eqs. (2.12), one finds that the real part of the poles are given by the solutions of the equation

$$(E-\tilde{E}_a)(E-\tilde{E}_c)-\underline{R}_{ac}\underline{R}_{ca} + (E-\tilde{E}_a)(E-\tilde{E}_c)/\{4[E-\tfrac{1}{2}(\tilde{E}_a+\tilde{E}_c)]^2\} \times(\Gamma_{aa}-\Gamma_{cc})^2=0, \quad \text{(A1)}$$

where all the quantities have been already defined in Eqs. (2.13a)–(2.13c). In general, Eq. (A1) is written in terms of complicated functions of E but at low intensity it can be reduced to a fourth-order equation if $\tilde{E}_i(E,\Gamma)\to\tilde{E}_i(E_i,\Gamma_{ii})$, $\Gamma_{ii}(E,\Gamma)$

$\to \Gamma_i(E_i, \Gamma_{ii})$, and $R_{ac}(E, \Gamma) \to R_{ac}(E_a, \Gamma_{aa})$.

By introducing the functions

$$F(E) = 1 + (\Gamma_{aa} - \Gamma_{cc})^2/4[E - \tfrac{1}{2}(E_a + E_c)]^2 , \quad \text{(A2a)}$$

and

$$G(E) = \underline{R}_{ac}\underline{R}_{ca}/(E - \tilde{E}_a)(E - \tilde{E}_c) . \quad \text{(A2b)}$$

Equation (A1) reads

$$F(E) - G(E) = 0 . \quad \text{(A3)}$$

In other words the solutions of Eq. (A1) are given by the crossing of the curves representing the functions $F(E)$ and $G(E)$. It is straightforward to show that these curves have only two crossing points. Thus Eq. (A1) has only two solutions.

To get approximate values for the complex poles it is preferable to start from

$$(z - z_a)(z - z_c) - \underline{R}_{ac}\underline{R}_{ca} = 0 , \quad \text{(A4)}$$

where

$$z_a = \tilde{E}_a - i\Gamma_{aa} , \quad \text{(A5a)}$$

$$z_c = \tilde{E}_c - i\Gamma_{cc} . \quad \text{(A5b)}$$

Owing to the obvious relation

$$(a + ib)^{1/2} = \frac{(a^2 + b^2)^{1/4}}{\sqrt{2}} \left\{ \left[1 + \frac{a}{(a^2 + b^2)^{1/2}} \right]^{1/2} + i \left[1 - \frac{a}{(a^2 + b^2)^{1/2}} \right]^{1/2} \right\} , \quad \text{(A6)}$$

the solutions of Eq. (A4) are found to be

$$z^{\pm} = \tfrac{1}{2}[\tilde{E}_a + \tilde{E}_c - i(\Gamma_{aa} + \Gamma_{cc})] \pm (1/\sqrt{2})(D_{ac}^2 + Q_{ac}^2)^{1/4} \times \left\{ \left[1 + \frac{D_{ac}}{(D_{ac}^2 + Q_{ac}^2)^{1/2}} \right]^{1/2} + i \left[1 - \frac{D_{ac}}{(D_{ac}^2 + Q_{ac}^2)^{1/2}} \right]^{1/2} \right\} , \quad \text{(A7)}$$

where

$$D_{ac} = \tfrac{1}{4}(\tilde{E}_a - \tilde{E}_c)^2 - \tfrac{1}{4}(\Gamma_{aa} - \Gamma_{cc})^2 + \underline{R}_{ac}\underline{R}_{ca} \quad \text{(A8a)}$$

and

$$Q_{ac} = -\tfrac{1}{2}(\tilde{E}_a - \tilde{E}_c)(\Gamma_{aa} - \Gamma_{cc}) . \quad \text{(A8b)}$$

At the crossing (anticrossing) point ($\tilde{E}_a = \tilde{E}_c$) the above expressions simplify. It is useful to know in this case the analytic expression of the transition probability we derive now.

(i) $(\Gamma_{aa} - \Gamma_{cc})^2 < 4\underline{R}_{ac}\underline{R}_{ca}$.

From Eq. (2.14b) one readily verifies that

$$\Gamma^+ = \Gamma^- = \tfrac{1}{2}(\Gamma_{aa} + \Gamma_{cc}) . \quad \text{(A9)}$$

On the other hand,

$$\Delta^+ = \Delta^- , \quad \text{(A10)}$$

$$D_{ac} = \underline{R}_{ac}\underline{R}_{ca} - [\tfrac{1}{2}(\Gamma_{aa} - \Gamma_{cc})]^2 , \quad \text{(A11)}$$

and

$$Q_{ac} = 0 . \quad \text{(A12)}$$

By using Eqs. (2.14a) and (2.18), one has

$$E^+ - E^- = 2(D_{ac})^{1/2} , \quad \text{(A13)}$$

$$\Omega^{\pm} = \pm (D_{ac})^{1/2} , \quad \text{(A14)}$$

and

$$\gamma_{cc}^+ = \gamma_{cc}^- \simeq \tfrac{1}{2}(\Gamma_{aa} - \Gamma_{cc}) . \quad \text{(A15)}$$

Therefore, the expression of the transition probability reduces to

$$P_M(t) = 1 - \frac{e^{-(\Gamma_{aa} + \Gamma_{cc})t}}{4\underline{R}_{ac}\underline{R}_{ca} - (\Gamma_{aa} - \Gamma_{cc})^2} \{ 4\underline{R}_{ac}\underline{R}_{ca} - (\Gamma_{aa} - \Gamma_{cc})^2 \cos[4\underline{R}_{ac}\underline{R}_{ca} - (\Gamma_{aa} - \Gamma_{cc})^2]^{1/2} t - (\Gamma_{aa} - \Gamma_{cc})[4\underline{R}_{ac}\underline{R}_{ca} - (\Gamma_{aa} - \Gamma_{cc})^2]^{1/2} \sin[4\underline{R}_{ac}\underline{R}_{ca} - (\Gamma_{aa} - \Gamma_{cc})^2]^{1/2} t \} \quad \text{(A16)}$$

(ii) $(\Gamma_{aa} - \Gamma_{cc})^2 > 4\underline{R}_{ac}\underline{R}_{ca}$.

In this case one finds

$$\Delta^+ = \Delta^- , \quad \text{(A17)}$$

$$D_{ac} = [\tfrac{1}{2}(\Gamma_{aa} - \Gamma_{cc})]^2 - \underline{R}_{ac}\underline{R}_{ca} , \quad \text{(A18)}$$

and

$$Q_{ac} = 0 . \quad \text{(A19)}$$

From Eqs. (2.14a) and (2.18) one finds

$$E^+ - E^- = 0 , \quad \text{(A20)}$$

$$\Omega^{\pm} = 0 , \quad \text{(A21)}$$

and

$$\gamma_{cc}^{\pm} = \tfrac{1}{2}(\Gamma_{aa} - \Gamma_{cc}) \pm (D_{ac})^{1/2} . \quad \text{(A22)}$$

The transition probability is given by

$$P_M(t) = 1 - \frac{e^{-(\Gamma_{aa} + \Gamma_{cc})t}}{(\Gamma_{aa} - \Gamma_{cc})^2 - 4\underline{R}_{ac}\underline{R}_{ca}} \{ -4\underline{R}_{ac}\underline{R}_{ca} + (\Gamma_{aa} - \Gamma_{cc})^2 \cosh[(\Gamma_{aa} - \Gamma_{cc})^2 - 4\underline{R}_{ac}R_{ca}]^{1/2} t - (\Gamma_{aa} - \Gamma_{cc})[(\Gamma_{aa} - \Gamma_{cc})^2 - 4\underline{R}_{ac}\underline{R}_{ca}]^{1/2} \sinh[(\Gamma_{aa} - \Gamma_{cc})^2 - 4\underline{R}_{ac}\underline{R}_{ca}]^{1/2} t \} . \quad \text{(A23)}$$

APPENDIX B

In what follows we give an illustration of the calculations whose results are reported in this paper. The simple example of one-photon bound-bound transition is considered. The generalization to N-photon processes is straightforward. It will be shown how the whole contribution of the continuum is taken into account.

The matrix $G(z)$ accounting for this one-photon process is given by

$$G(z)=\begin{pmatrix} E-E_a-R_{aa}(z) & -R_{ab}(z) \\ -R_{ba}(z) & E-E_b-E_{bb}(z) \end{pmatrix}^{-1}, \tag{B1}$$

where the energies of the system atom plus field are given in terms of the atomic energies E_1 and E_2 by

$$E_a=E_1+n\omega, \tag{B2a}$$

$$E_b=E_2+(n-1)\omega. \tag{B2b}$$

The expressions for the matrix elements of $R(z)$ occurring in Eq. (B1) can be found from Eqs. (2.6) and (2.7). In focusing our attention on R_{ba} and R_{bb} one finds that

$$R_{ba}(z)=\langle b|\,(V^+\bar{\tau}_{\square}\bar{A}\bar{\tau}_0\bar{A}\bar{\tau}_0+V^-\bar{\tau}_{\square})|\,a\rangle, \tag{B3a}$$

$$R_{bb}(z)=\langle b|(V^+\bar{\tau}_{\square}\bar{A}\bar{\tau}_0+V^-\bar{\tau}_{\square}\bar{B}\bar{\tau}_0)|\,b\rangle, \tag{B3a}$$

which, by virtue of Eq. (2.7), become

$$R_{ba}=\langle 2,n-1|\,V^+\frac{1}{1-\bar{A}\dfrac{1}{1-\bar{A}\cdots\bar{B}}\bar{B}-\bar{B}\dfrac{1}{1-\bar{B}\cdots\bar{A}}\bar{A}}\bar{A}\frac{1}{1-\bar{A}\dfrac{1}{1-\bar{A}\cdots\bar{B}}\bar{B}}\bar{A}\frac{1}{1-\bar{A}\dfrac{1}{1-\bar{A}\cdots\bar{B}}\bar{B}}|\,1,n\rangle$$

$$+\langle 2,n-1|\,V^-\frac{1}{1-\bar{A}\dfrac{1}{1-\bar{A}\cdots\bar{B}}\bar{B}-\bar{B}\dfrac{1}{1-\bar{B}\cdots\bar{A}}\bar{A}}|\,1,n\rangle, \tag{B4a}$$

$$R_{bb}=\langle 2,n-1|\,V^+\frac{1}{1-\bar{A}\dfrac{1}{1-\bar{A}\cdots\bar{B}}\bar{B}-\bar{B}\dfrac{1}{1-\bar{B}\cdots\bar{A}}\bar{A}}\bar{A}\frac{1}{1-\bar{A}\dfrac{1}{1-\bar{A}\cdots\bar{B}}\bar{B}}|\,2,n-1\rangle$$

$$+\langle 2,n-1|\,V^-\frac{1}{1-\bar{A}\dfrac{1}{1-\bar{A}\cdots\bar{B}}\bar{B}-\bar{B}\dfrac{1}{1-\bar{B}\cdots\bar{A}}\bar{A}}\bar{B}\frac{1}{1-\bar{B}\dfrac{1}{1-\bar{B}\cdots\bar{A}}\bar{A}}|\,2,n-1\rangle, \tag{B4b}$$

where the standard notation has been adopted for the states of the system. Let d be the dipole operator, one defines

$$\bar{d}^n=[Q/(E-H_A^0-n\omega)]d, \tag{B5}$$

where Q is the projector outside the two-dimensional space spanned by the states $|\,a\rangle$ and $|\,b\rangle$ and H_A^0 is the free-energy operator for the atom.

Owing to the relations

$$\bar{A}=\bar{d}a, \tag{B6}$$

$$\bar{B}=\bar{d}a^+,$$

and

$$a|\,n\rangle=\sqrt{n}\,|\,n-1\rangle, \qquad a^+|\,n\rangle=\sqrt{n+1}\,|\,n+1\rangle, \tag{B7}$$

Eq. (B4) can be written, in the dipole approximation, as

$$R_{ba}=(n-1)\sqrt{n}<2|\,d\frac{1}{1-(n-1)\bar{d}^{n-2}\dfrac{1}{1-n\bar{d}^{n-1}\cdots\bar{d}^n}\bar{d}^{n-1}-(n-2)\bar{d}^{n-2}\dfrac{1}{1-(n-3)\bar{d}^{n-3}\cdots\bar{d}^{n-4}}\bar{d}^{n-3}}\bar{d}^{n-2}$$

$$\times\frac{1}{1-n\bar{d}^{n-1}\dfrac{1}{1-(n+1)\bar{d}^n\cdots\bar{d}^{n+1}}\bar{d}^n}\bar{d}^{n-1}\frac{1}{1-(n+1)\bar{d}^n\dfrac{1}{1-(n+2)\bar{d}^{n+1}\cdots\bar{d}^{n+2}}\bar{d}^{n+1}}|\,1\rangle$$

$$+\sqrt{n}<2|\,d\frac{1}{1-(n+1)\bar{d}^n\dfrac{1}{1-(n+2)\bar{d}^{n+1}\cdots\bar{d}^{n+2}}\bar{d}^{n+1}-n\bar{d}^n\dfrac{1}{1-(n-1)\bar{d}^{n-1}\cdots\bar{d}^{n-2}}\bar{d}^{n-1}}|\,1\rangle, \tag{B8a}$$

$$R_{bb}=(n-1)\langle 2|\,d\frac{1}{1-(n-1)\bar{d}^{n-2}\dfrac{1}{1-n\bar{d}^{n-1}\cdots\bar{d}^{n}}\bar{d}^{n-1}-(n-2)\bar{d}^{n-2}\dfrac{1}{1-(n-3)\bar{d}^{n-3}\cdots\bar{d}^{n-4}}\bar{d}^{n-3}}\bar{d}^{n-2}$$

$$\times\frac{1}{1-n\bar{d}^{n-1}\dfrac{1}{1-(n+1)\bar{d}^{n}\cdots\bar{d}^{n+1}}\bar{d}^{n}}|2\rangle$$

$$+n\langle 2|\,d\frac{1}{1-(n+1)\bar{d}^{n}\dfrac{1}{1-(n+2)\bar{d}^{n+1}\cdots\bar{d}^{n+2}}\bar{d}^{n+1}-n\bar{d}^{n}\dfrac{1}{1-(n-1)\bar{d}^{n-1}\cdots\bar{d}^{n-2}}\bar{d}^{n-1}}\bar{d}^{n}$$

$$\times\frac{1}{1-(n-1)\bar{d}^{n-1}\dfrac{1}{1-(n-2)\bar{d}^{n-2}\cdots\bar{d}^{n-3}}\bar{d}^{n-2}}|2\rangle\,. \tag{B8b}$$

It is clear from Eqs. (B8) that it is not necessary to calculate separately all the continued fractions appearing in the expressions of R_{ba} and R_{bb}. This is due to the fact that the same continued fraction appears many times. This general property exhibited by the ensemble of expressions discussed so far is in intensively used to shorten the needed computer time. To determine the place where the integration over the continuum variables must be performed, we consider a continuum discretized with two states. This is an artifact. It is understood that the integral over the continuum is symbolized everywhere by the sum over these two states. We choose a particular set of atomic states. $|1\rangle$ and $|2\rangle$ are the two discrete states already mentioned whereas the continuum is discretized by the states $|3\rangle$ and $|4\rangle$ in such a way that the only allowed transitions are $|1\rangle \rightleftharpoons |2\rangle$ and $|2\rangle \rightleftharpoons (|3\rangle, |4\rangle)$.

In this case Eqs. (B8a) and (B8b) reduce to

$$R_{ba}=\sqrt{n}d_{21}\,, \tag{B9a}$$

$$R_{bb}=n\langle 2|\,d\frac{1}{1-n\bar{d}^{-2}\dfrac{1}{1-n\bar{d}^{-3}\cdots\bar{d}^{-4}}\bar{d}^{-3}}\bar{d}^{-2}|2\rangle\,, \tag{B9b}$$

where, for shortness, n has been subtracted from all the superscripts and the depletion of the photons has been neglected, i.e., $n\gg 1$.

The particularly simple form of Eqs. (B9) is a consequence of the projector Q.

In the basis we consider, the dipole operator is represented by the matrix

$$d=\begin{bmatrix}0 & d_{12} & 0 & 0\\ d_{21} & 0 & d_{23} & d_{24}\\ 0 & d_{32} & 0 & 0\\ 0 & d_{42} & 0 & 0\end{bmatrix}. \tag{B10}$$

By using Eq. (B5) it is a simple matter to calculate R_{bb} as given by Eq. (B9b). Limiting ourselves to a single interaction in Eq. (B9b) one has

$$R_{bb}=n\langle 2|\,\bar{d}^{-2}D^{-1}d|\,2\rangle\,, \tag{B11}$$

where D^{-1} is the inverse of the matrix

$$D=1-n\bar{d}^{-2}\bar{d}^{-3}\,. \tag{B12}$$

By introducing the completeness relation

$$\sum_{i=1}^{4}|i\rangle\langle i|=1 \tag{B13}$$

in Eq. (B11) one sees how the continuum indices of D^{-1} and d are to be integrated.

The same discussion holds for the continuum indices appearing in the expression of the matrix elements of D^{-1}. To see this we consider the diagonal matrix element D_{22}^{-1}. One easily finds that

$$D_{22}^{-1}=1/[1-n(\bar{d}^{-2}\bar{d}^{-3})_{22}]\,. \tag{B14}$$

As before it is clear that an integration over the inner continuum indices of the product of matrices $\bar{d}^{-2}\bar{d}^{-3}$ is to be done. As a general rule one must integrate over the inner repeated continuum indices appearing at every stage of iteration in the continued fractions.

[1]See H. B. Bebb and A. Gold, Phys. Rev. 143, 1 (1966); P. Lambropoulos, Phys. Rev. A 9, 1992 (1974); Y. Gontier and M. Trahin, Phys. Rev. A 4, 1896 (1971), and the references quoted therein.

[2]Y. Gontier, N.K. Rahman, and M. Trahin, Phys. Rev. A 14, 2109 (1976).

[3]C. Cohen-Tannoudji, *Cargese Lectures in Physics*, edited by M. Levy (Gordon and Breach, New York, 1967), Vol. 2, pp. 347–393. C. Cohen-Tannoudji and S. Haroche, J. Phys. (Paris) 30, 125 (1969); 30,

153 (1969).
[4]L. Mower, Phys. Rev. 142, 799 (1966).
[5]M. L. Goldberger and K. M. Watson, *Collision Theory* (Wiley, New York, 1964), Chap. 8.
[6]B. L. Beers and L. Armstrong, Jr., Phys. Rev. A 12, 2447 (1975). The method of effective Hamiltonian used by these authors has also been utilized in S. Feneuille and L. Armstrong Jr., J. Phys. (Paris) 36, L235 (1975) and in L. Armstrong Jr., B. Beers, and S. Feneuille, Phys. Rev. A 12, 1903 (1975).
[7]A. T. Georges and P. Lambropoulos, Phys. Rev. A 15, 727 (1977).
[8]B. W. Shore and J. Ackerhalt, Phys. Rev. A 15, 1640 (1977).
[9]G. Brincourt, J. Phys. (Paris) 38, L81 (1977).
[10]J.Morellec, D. Normand, and G. Petite, Phys. Rev. A 14, 300 (1976).
[11]L. A. Lompre, G Mainfray, C. Manus, and J. Thebault, J. Phys. (Paris) 39, 610 (1978).
[12]B. Warner, Mon. Not. R. Astron. Soc. 139, 115 (1968).
[13]M. Crance and S. Feneuille, Phys. Rev. A 16, 1587 (1977). In this paper the authors give the value of the ionization cross section from the 6*f* level calculated by M. Aymar.
[14]Y. Gontier and M. Trahin, Phys. Lett. A 63, 165 (1977).
[15]E. Courtens and A. Szöke, Phys. Rev. A 15, 1588 (1977).
[16]Y. Gontier and M. Trahin, Phys. Rev. A 7, 1899 (1973).
[17]C. S. Chang and P. Stehle, Phys. Rev. Lett. 30, 1283 (1973).